PERGAMON

Solid-State Electronics 44 (2000) 631–638

SOLID-STATE ELECTRONICS

Characteristics of high breakdown voltage Schottky barrier diodes using p^+-polycrystalline-silicon diffused-guard-ring

Bor Wen Liou[a,*], Chung Len Lee[b]

[a]*Department of Electrical Engineering, Wu-Feng Jr. College of Technology and Commerce, 117 Chian-Ku Rd, Sec. 2, Chiayi, Taiwan, Republic of China*

[b]*Department of Electronics Engineering and Institute of Electronics, National Chiao Tung University, 1001 Ta Hsueh Rd, Hsinchu, Taiwan, Republic of China*

Received 17 May 1999; received in revised form 14 July 1999; accepted 16 September 1999

Abstract

A new structure of Schottky diode using the p^+-polycrystalline silicon (polysilicon) diffused-guard-ring is proposed. For 950°C with 30 min annealing condition, the diode gives a nearly ideal *J–V* characteristic with a high reverse breakdown voltage (148 V) and a low reverse leakage current density (8.4 μA/cm^2). The guard-ring structure prevents the premature breakdown; the polysilicon layer prevents the surface leakage. It was also found that the more the driving time of furnace, the higher the breakdown voltage of the Schottky diode. The breakdown characteristic of a Schottky diode was shown to be closely related with the diffusion length of the boron ions being inside the Si wafer. The electrical characteristics of the p^+-polysilicon diffused-guard-ring Schottky device was compared with those of the conventional diffused-guard-ring sample. © 2000 Published by Elsevier Science Ltd. All rights reserved.

1. Introduction

It is interesting that the Schottky diode, a majority carrier device, in which there is virtually no minority carrier storage, opens up a wide avenue of high-speed applications. It is essential to use the power rectifier with the high speed-switching capability. In comparison, the conventional silicon rectifier has a low breakdown voltage because of its excessive reverse leakage current and of its limiting forward conduction current-handing capability with increasing breakdown voltage [1]. Hence, the epitaxial silicon wafer will be used for application of the high-power device in the future. Although a true reverse leakage current of the metal–semiconductor (Schottky) device has been difficult to interpret in theory, the diffused-guard-ring structure can eliminate the premature breakdown and give a low leakage current [2,3]. Moreover, the overlap-metal structure [4] gives a near-ideal forward *I–V* characteristic and has a low leakage current density under the moderate reverse bias. Recently, many structures have been proposed [5] to prevent the electrode sharp-edge effect of the diode and give ideal forward and reverse characteristics. Similarly, the reverse direction of the polysilicon emitter (poly-emitter) diode of the p–n junction generally exhibits a lower leakage current and a higher breakdown voltage as compared to a conventional-Schottky diode [2,6]. Hence, we propose a new

* Corresponding author. Tel.: +886-5-226-7125-2531; fax: +886-5-226-4224.

E-mail addresses: bwliu@snu5.wfc.edu.tw (B.W. Liou), cllee@cc.nctu.edu.tw (C.L. Lee).

PII: S0038-1101(99)00258-0

structure in this experiment, which can combine the advantage of a high reverse breakdown voltage of the poly-emitter structure with a fast response of the Schottky diode with the diffused-guard-ring structure. The guard-ring structure of heavily doped polysilicon with a polysilicon-overlap structure onto the epitaxial wafer was used to demonstrate in this experiment. It was found that this new device not only took a low leakage current and high reverse breakdown voltage, but also maintained the advantage of the Schottky barrier. This fabricated device indeed demonstrates for the feature. In comparison, the conventional Schottky diode of diffused guard-ring with the metal-overall structure and the poly-emitter diode was also investigated together. Furthermore, the native-oxide impact of polysilicon/mono-silicon interface was also studied together with this structure [7].

2. Experimental procedure

Since the investigation was mad to improve the understanding of the polysilicon overlap and guarding-ring structure can improve the breakdown voltage of Schottky diode. Four different types of diodes were studied together and are depicted in Fig. 1. In Fig. 1(a), a conventional-planar-Schottky barrier employing the metal overlap is referred to as diode A. In Fig. 1(b), the p^+ diffused-guarding diode without polysilicon overlap is referred to as diode B. Fig. 1(c) shows a poly-emitter diode employing a polysilicon layer with polysilicon–metal overlap, which is referred to as diode C [6]. Finally, in Fig. 1(d), the proposed diode by using the guard-ring diode of p^+-polysilicon-diffused with the 25 μm polysilicon guarding-ring and 30 μm polysilicon-overlap length, hereafter referred to as diode D. The wafer used is a n-type 0.01 Ω cm ⟨100⟩ wafer with a 20 μm thick epitaxial layer ⟨100⟩ orientation whose resistivity of the epi-layer was 10 Ω cm. Fig. 2 (a) is a process-flow chart of four-diode fabrication and Fig. 2(b) is a sequential process step of proposed diode D. The fabricated-process sequence is as follows: first, the wafer was cleaned by RCA process sequence and the SiO_2 layer of approximately 7000 Å was grown at 1100°C, wet oxygen for 1 h; then defined the guard-ring pattern of the oxide film. However, diode C did not define the guard-ring pattern and used the metal film to directly contact onto the polysilicon

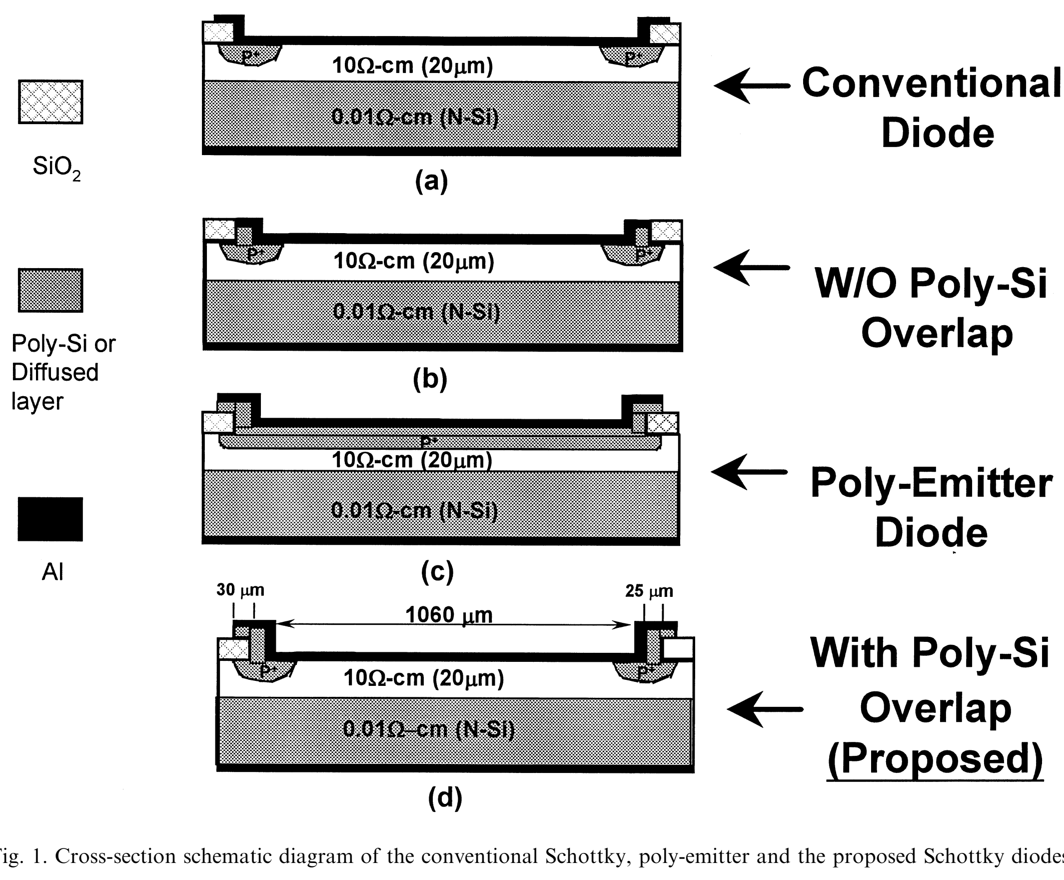

Fig. 1. Cross-section schematic diagram of the conventional Schottky, poly-emitter and the proposed Schottky diodes.

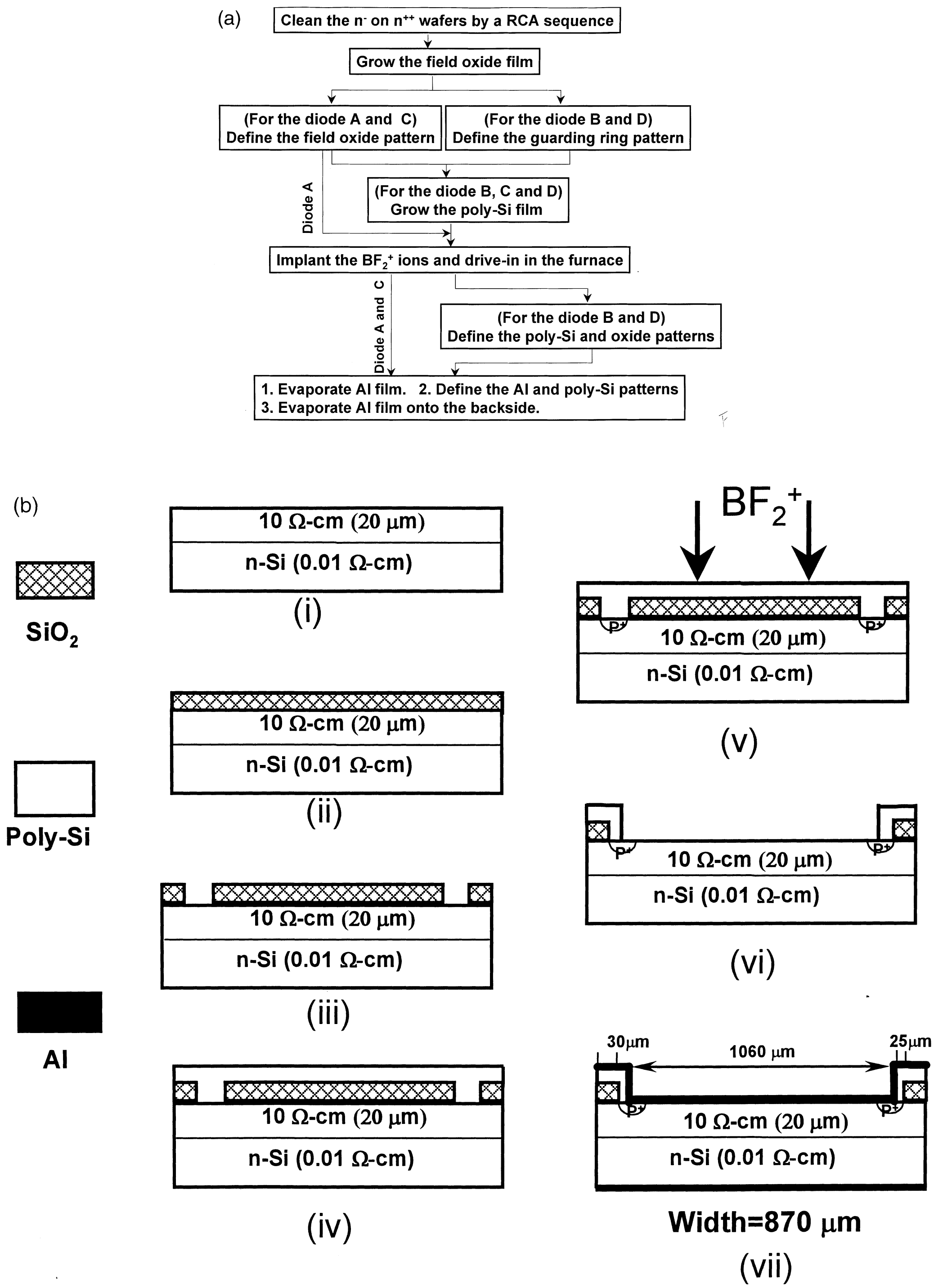

Fig. 2. (a) The process-flow chart of four-diodes fabrication. (b) The process steps of the proposed diode D fabrication.

film surface. Next, the undoped polysilicon (or amorphous) film of 3000 Å was deposited in a LPCVD (lower pressure chemical vapor deposition) reactor at 625°C (or 550°C) with SiH_4 gas under a pressure of 100 mTorr [6]. The H_2SO_4 sample was cleaned by H_2SO_4:H_2O_2 (3:1) solution before the polysilicon layer was deposited; likewise, the HF sample was dipped in dilute HF (1:50) solution for 40–50 s before the polysilicon layer was deposited [8,9,16]. Thus, the H_2SO_4 sample exhibited a thin native oxide film (< 20 Å) at the polysilicon/mono-silicon interface [9]. Following this, the conventional diode of Fig. 1 (a) was implanted by BF_2^+ at 40 keV with a dosage of 1×10^{16} cm^{-2}. The structures of the diodes depicted in Fig.1(b–d) received the BF_2^+ implantation at 120 keV with a dosage of 1×10^{16} cm^{-2}. After implantation, all the samples were annealed at 950°C with 30–210 min in N_2 gas. Then diodes B and D were used for the standard photo-resist technique to form the polysilicon-guard-ring structure. Before the metal deposition, all the wafers were chemically cleaned by a RCA sequence and finally rinsed in a dilute HF solution. Finally, all the samples were formed by thermal evaporation of the Al film (with 1% Si), sequentially sintered at 400° C for 30 min in N_2 gas and the devices were patterned to define. The Keithley 237 and Keithley 590 equipment measured the current–voltage characteristic and the capacitance–voltage curve, respectively. The junction depth of boron ions was measured by the SRP (spreading resistance profiling) technique of the SSM (Solid State Measurements) Company.

3. Results and discussion

3.1. Forward J–V characteristics

Fig. 3 shows the measured forward *J–V* characteristics of four different structures (diodes A–D) with HF and H_2SO_4, respectively. In this figure, several facts can be observed: (1) the current density of diode A was less than that of diode D and diodes A and D exhibited a three logarithmic-decade difference; (2) the conventional diode exhibited the lowest effective barrier height ($\phi_{bn} \approx 0.73$ eV) as compared to the other diodes; (3) the poly-emitter diode C had a good ideality factor ($n \approx 1.002$) for the 10 logarithmic-linear decades; (4) the guard-ring structure of diode D exhibits a near-ideal forward characteristic and a high driving current density. The ideality factor, n, was about 1.07 for seven logarithmic decades and the forward current density was about 30 A/cm^2 at 0.6 V; and (5) the effective barrier height of the Schottky diode with native oxide was lightly greater than that of the without-native-oxide sample. The effective barrier height, ideality factor and breakdown leakage current density J_{bd} of these diodes are given together in Table 1. Because the native oxide of polysilicon/mono-silicon could block the minority carrier into the polysilicon film, so that the effective barrier height of the HF diode (0.75 eV) is slightly smaller than that of the H_2SO_4 (0.76 eV) sample; likewise, the forward current of all diodes with the H_2SO_4 sample was also slightly smaller than that of the HF sample. Similarly, the forward current of

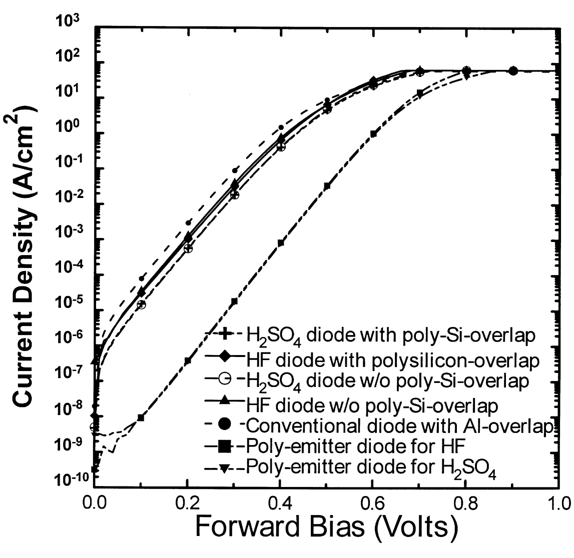

Fig. 3. Forward current density versus applied voltage of the fabricated diodes and poly-emitter diodes. The polysilicon film was ADP structure. The furnace temperature was 950°C and drive-in time was set at 30 min.

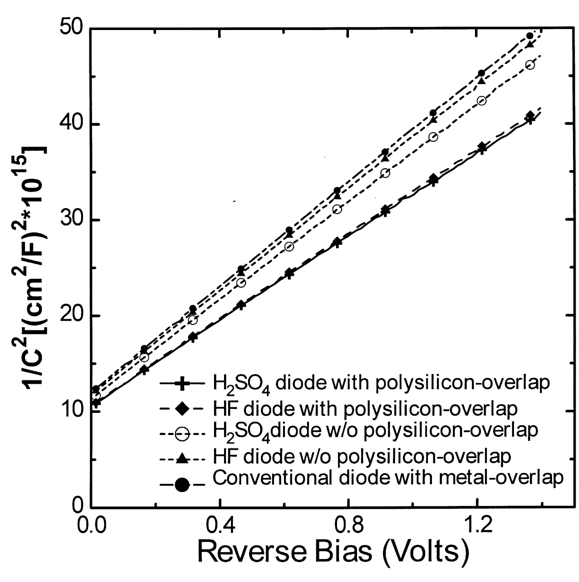

Fig. 4. $1/C^2$ versus applied voltages for fabricated diodes. The polysilicon film was of ADP structure. The furnace temperature was 950°C and drive-in time 30 min.

diode D was lightly smaller than that of diode B under the same forward bias. On the other hand, this forward current of the diode D consists of two components: one is a pure Schottky barrier current and another is a p^+/n guard-ring junction current. Moreover, the forward current of the poly-emitter diode was much smaller as compared to the Schottky barrier diode, as shown in Fig. 3. Hence, we can conclude that the forward current of the Schottky diode with p^+-polysilicon-diffused guard-ring dominated by the Schottky barrier current.

3.2. Capacitance–voltage characteristics

The capacitance–voltage characteristics were measured at 100 kHz. Fig. 4 shows the data of C^{-2} versus the reverse bias. The dopant concentration of the Schottky diode was also measured using the slope of the C^{-2}–V curve. From Fig. 4, the obtained value of the effective carrier concentration is very consistent with the initial-growth doping level ($\cong 4.8 \times 10^{14}$ cm^{-3}) of epi-wafer. Furthermore, it was due to the effect of the barrier height lowering of the J–V measurement technique; as expected, the effective barrier height of diode D (H_2SO_4 sample) was lightly smaller than the value of 0.76 eV, as determined by C–V measurement [10]. The measured C–V barrier heights of the other diodes were also given in Table 1. For example, ϕ_{bn} of diode A was about 0.74 eV; ϕ_{bn} of diode B was about 0.75 and 0.74 eV for the H_2SO_4 and HF samples, respectively. Likewise, ϕ_{bn} of diode D was about 0.76 eV. It can be observed that the effective barrier height and the reverse-breakdown voltage of the H_2SO_4 sample were lightly greater than those of the HF sample. This result was consistent with the previous mentioned, where the reverse-breakdown voltage of diode is depended upon the barrier height of the metal–semiconductor (MS) contact.

3.3. Reverse J–V characteristics

The reverse characteristics of p^+-polysilicon Schottky barrier diodes are given in Fig. 5, which shows the 950°C, 30 min annealing condition. Fig. 5 (a) is the as-deposition polysilicon (ADP) diode and Fig. 5 (b) is the stacked-amorphous silicon (SAS) diode [6]. As can be seen in Fig. 5 (a), the breakdown voltage of the conventional p^+-n diffused guard-ring diode is about 25 V and its reverse leakage current density about 0.33 mA/cm^2. A low breakdown voltage and a great reverse leakage current may be due to the premature edge breakdown of diode. Next, for the p^+-polysilicon diffused-guard-ring diode without the overlap metal (diode B), the breakdown voltages are 68 and 73 V for the HF and the H_2SO_4 sample, respectively. For the p^+-polysilicon diffused-guard-ring diode with the polysilicon-overlap structure (diode D), the breakdown voltage of HF sample is about 148 V and its reverse leakage current density about 19.5 μA/cm^2. Likewise, the H_2SO_4 sample had a higher breakdown voltage ($\cong$149 V) and a lower leakage current ($\cong$8.4 μA/cm^2) as compared to the HF sample. This reduction can be attributed to the presence of the native oxide layer, which blocks the minority-carrier injection into the polysilicon layer. As a result, the electron–hole pair recombination at grain boundaries of the polysilicon film and in the interior of the polysilicon grains would be reduced. Bravman [11] has already shown that the interfacial native oxide layer could avoid the breaking of the polysilicon film. This extension of epi-regrowth at the poly-Si/mono-Si interface increases with the increase of annealing temperature and drive-in time [12–15]. This result might cause the interface of poly-Si/mono-Si to look very rough [14]. Then the native oxide of the H_2SO_4 sample could inhibit more epi-regrowth of this interface as compared to the HF-dip sample [11]. Their breakdown voltage and leakage-current density are also given in Table 1. From this result, we can conclude that the polysilicon diffused-guard-ring can improve the electrical field

Table 1
The electrical characteristics of diode A–D. It shows the reverse current density, reverse breakdown voltage, barrier height and ideality factor

	J_r (μA/cm^2) at $V_r = 50$ V	J_r (μA/cm^2) at $V_r = 65$ V	V_{bd} (V)	J_{bd} (μA/cm^2)	ϕ_{bn} (eV) by J–V	ϕ_{bn} (eV) by C–V	n
Diode A (C.S.)	–	–	25	332	0.734	0.740	1.100
Diode B (H_2SO_4)	4.68	6.61	73	24.2	0.742	0.746	1.080
Diode B (HF)	2.59	3.18	68	6.04	0.741	0.744	1.090
Diode C (H_2SO_4)	1.85×10^{-3}	2.27×10^{-3}	159	3.72×10^{-3}	–	–	1.002
Diode C (HF)	2.25×10^{-3}	2.67×10^{-3}	156	4.47×10^{-3}	–	–	1.004
Diode D (H_2SO_4)	1.96	2.32	149	8.4	0.757	0.760	1.070
Diode D (HF)	2.59	3.18	148	19.5	0.753	0.758	1.070

limitation, the overlap-polysilicon sample could suppress the edge electrical field and the breakdown voltage of the H_2SO_4 sample is slightly greater than that of the HF sample.

From Table 1, for the H_2SO_4 sample, the breakdown voltage of diode A was 25, of diode B 73.5 and of diode D about 149 V. The reverse leakage current could increase with the decrease of contact area of overlap metal or polysilicon layer. Thus, this could cause the diode to exhibit a low breakdown voltage. Therefore, the overlap-metal and/or -polysilicon sample exhibited a higher reverse breakdown voltage and a lower leakage current as compared to non-overlap-metal or -polysilicon sample, respectively.

Comparing the breakdown characteristic of the ADP and SAS structures, one can find that the breakdown voltage of the ADP structure is slightly greater than that of the SAS structure and the leakage current of the former is smaller as compared to the latter. For the 950°C annealing condition of furnace, the reverse breakdown voltage and boron-diffusion depth in terms of the drive-in time are given in Fig. 6. For example, for 30 min drive-in, the boron-diffused depth of the ADP structure is about 0.25 μm and for SAS about 0.21 μm [6]. On the other hand, the deeper the diffused length of the p^+/n guard-ring junction, the higher the reverse breakdown voltage. From the previous discussion of breakdown voltage of diode, it could be observed that the breakdown phenomenon occurred at the edge of the guard-ring of heavily doped polysilicon film. Thus, another method of improving the breakdown voltage was the increase of breakdown voltage of the p^+/n guard-ring junction. In addition, the reverse leakage current density of the p^+-polysilicon diffused-guard-ring Schottky diode was much smaller than that of the conventional Schottky sample. This result can be explained by the fact that the polysilicon-guard-ring structure could trap the mobile ions and the shallow-diffused junction could smooth the edge-electrical field. This effect made the guard-ring Schottky diode with the overlap-polysilicon structure

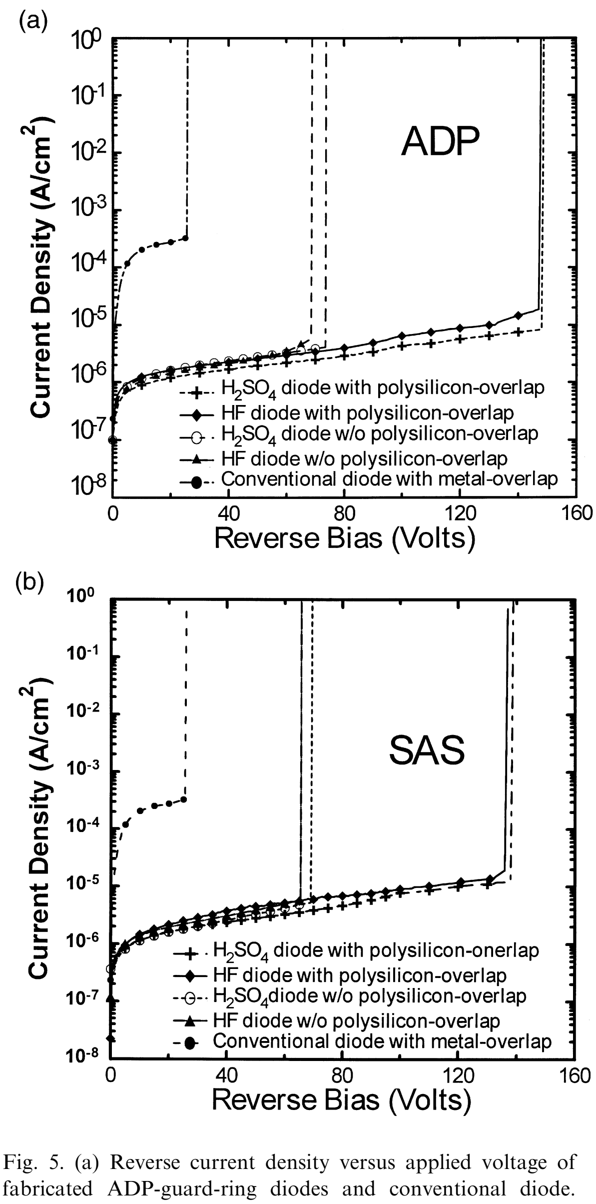

Fig. 5. (a) Reverse current density versus applied voltage of fabricated ADP-guard-ring diodes and conventional diode. The furnace temperature was 950°C and drive-in time 30 min. (b) Reverse current density versus applied voltage of fabricated SAS-guard-ring diodes. The furnace temperature was 950°C and drive-in time 30 min.

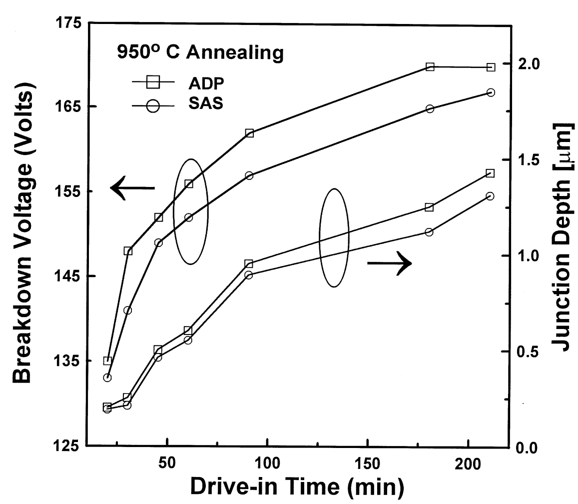

Fig. 6. Reverse J–V characteristics and boron diffusion length in terms of the drive-in time of furnace. It shows the ADP and SAS sample, respectively.

to inhibit the reverse leakage current and give a high breakdown voltage.

Fig. 7 shows the reverse characteristic of the poly-emitter diode with the ADP structure. The breakdown voltage of the H_2SO_4 sample is about 159 V and its reverse leakage current density about 3.72 nA/cm^2; similarly, the breakdown voltage of the HF sample is about 156 V and its leakage current density about 4.47 nA/m^2. This phenomenon can be similar to the result of a heavily doped polysilicon diode with polysilicon overlap that the breakdown voltage of H_2SO_4 sample was lightly greater as compared to the HF sample. The punch-through-breakdown voltage of 10 ± 1.5 Ω cm, 20 ± 3 μm epitaxial-layer wafer was about 174 V. No matter what the poly-emitter diode or p$^+$polysilicon diffused-guard-ring Schottky diode with polysilicon overlap, their breakdown voltages were very high and approached the ideal punch-through voltage of this raw epi-wafer substrate.

3.4. The statistical plots of breakdown voltages

Fig. 8 shows the statistical plots of the breakdown voltages of the ADP structure for three types of diode for each of the 30 diodes. For these data, the breakdown conditions were: furnace temperature 950°C and drive-in time 30 min. The conventional p$^+$–n guard-ring diode had a low breakdown voltage occupation; for example, the occupation of 25 V was about 60%. The guard-ring diode of heavily doped polysilicon had a higher breakdown voltage statistic as compared to the conventional diode. It is clearly shown that the polysilicon-overlap sample tended to have a higher breakdown voltage occupation as compared to a non-polysilicon-overlap sample. In Fig. 8(a), for diode D, the occupations of 150 V: the H_2SO_4 sample was 50% and the HF sample 20%; likewise, the occupation of 140 V: the H_2SO_4 sample was 15% and the HF sample 35%. This result can help us to explain that diode D

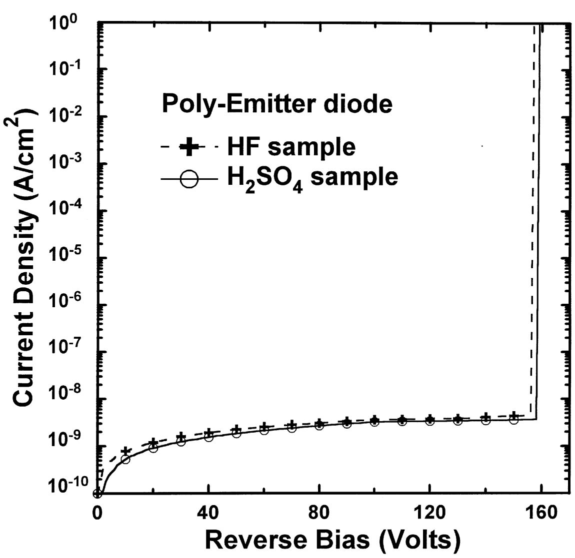

Fig. 7. Reverse current density versus applied voltage of poly-emitter diode. The polysilicon film was ADP structure. The furnace temperature was 950°C and drive-in time 30 min. It shows the H_2SO_4 and HF samples, respectively.

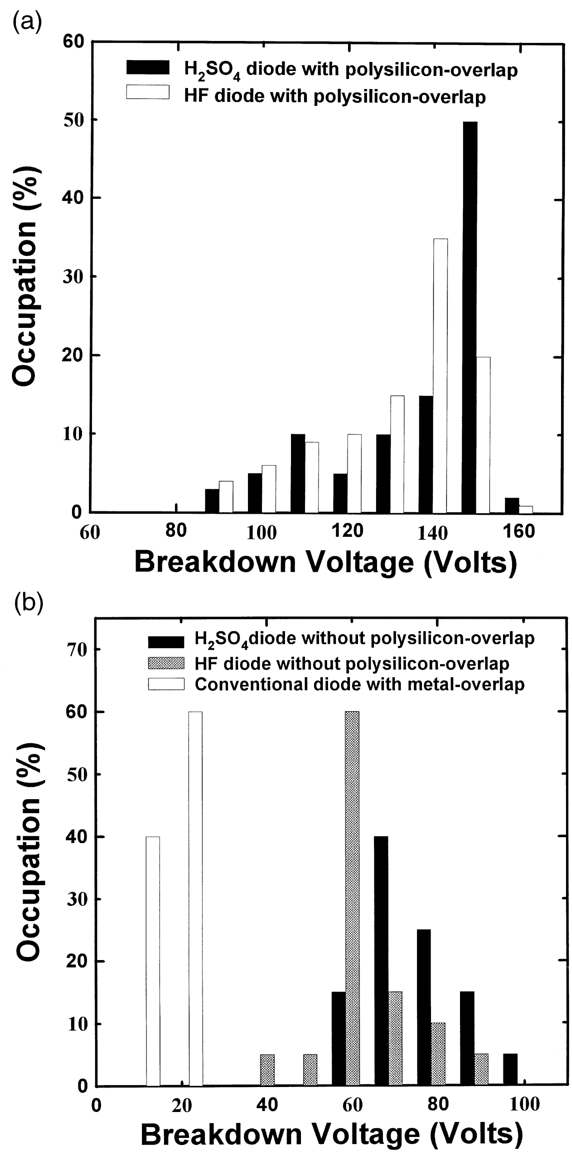

Fig. 8. (a) Statistical plots of reverse breakdown voltages for fabricated diodes with the polysilicon-overlap structure. (b) Statistical plots of reverse breakdown voltages for fabricated diodes without polysilicon/overlap and conventional structures.

was a higher barrier-height device as compared to the other diodes, as is previously mentioned. On the other hand, it can endure a strong electric field between the metal contact and the silicon substrate, which leads to a tough breakdown voltage. Therefore, the guard-ring structure of heavily doped polysilicon could prevent premature electrical breakdown around the periphery of the diode contact. The breakdown voltage phenomenon of the non-polysilicon-overlap structure and the conventional p^+–n guard-ring diode is shown in Fig. 8(b): the 60 V occupation of the HF sample is 65% and the 70 V occupation of the H_2SO_4 sample 40%. It is further observed that diode D had a greater breakdown voltage occupation as compared to diodes B and A. On the other hand, by joint applying the polysilicon-overlap, metal-overlap and diffused-guard-ring structure, a high performance Schottky diode with a high breakdown voltage and low leakage current can be achieved. Therefore, the fabricated device was found to demonstrate the above future.

4. Conclusions

This work has shown nearly ideal forward and higher reverse breakdown voltage characteristics of the proposed diode which obtains to use the heavily doped-polysilicon-guard-ring structure. A heavily doped polysilicon film can be applied to a Schottky barrier diode to form a polysilicon emitter guard-ring junction. Due to the high breakdown voltage of the polysilicon emitter diode of the guard-ring, a high breakdown voltage Schottky diode can be obtained. By comparing *J–V* characteristics of the conventional sample and the proposed sample, the following general behaviors can be observed:

1. For most of the practical Schottky diode, the dominant reverse current component is the edge-leakage current around the periphery of the metal plate. Therefore, leakage current decreases with the increase of the guard-ring area of heavily doped-polysilicon film. For the polysilicon-overlap sample, the shallow-diffused depth can smooth the edge electric field, and this result makes the breakdown voltage to be high and leakage current to be small.
2. The polysilicon-overlap diode D has a near-ideal forward *J–V* characteristic and a low leakage current at moderate reverse bias, in comparison, diode B exhibits a high reverse current density and a low breakdown voltage. Thus, the polysilicon-overlap structure can suppress the electrode sharp edge effect of diode.
3. The presence of native oxide layer at the polysilicon/mono-silicon interface can avoid the polysilicon film to break and block minority carrier injection. Thus, this effect makes the trapped density to decrease and improves the breakdown voltage of diode.
4. For the 950°C temperature annealing, the longer the drive-in time of furnace, the deeper the boron diffusion length, which causes the breakdown voltage of the diode to be high

.

Acknowledgements

The authors would like to acknowledge the technical support of the Vanguard International Semiconductor Corporation and financial support of National Science Council of R.O.C. through contract NSC-83-0404-E009-017 for this research.

References

[1] Henisch HK. Rectifying semiconductor contacts. Oxford Clarendon press, 1957.
[2] Liou BW, Lee CL, Lei TF. IEEE Electron Lett 1995;31:1950.
[3] Chang CY, Sze SM. Solid-State Electron 1970;13:727.
[4] Saltich JL, Clark LE. Solid-State Electron 1970;13:857.
[5] Andrews JM, Lepselter MP. Solid-State Electron 1970;13:1011.
[6] Wu SL, Lee CL, Lei TF, Chang HC. IEEE Trans Electron Devices 1993;40:1797.
[7] Neugroschel A, Arienzo M, Komem Y, Isaac RD. IEEE Trans Electron Devices 1985;32:807.
[8] Chu TL. J Cryst Growth 1977;39:45.
[9] Ashburn P, Soerowirdjo B. IEEE Trans Electron Devices 1984;31:853.
[10] Yang ES. Microelectric devices. McGraw international editions, 188, 1988.
[11] Bravman JC, Patton GL, Plummer JD. J Appl Phys 1985;57:2779.
[12] Jorgensen N, Barry JC, Booker GR., Ashburn P. Wolstenholme GR, Wilson MC and Hunt PC. In: Microscopy of semiconductor materials Conf. Dig. (Oxford, UK), 1985.
[13] Patton GL, Bravman JC, Plummer JD. IEEE Trans Electron Devices 1986;33:1754.
[14] Wolstenholme GR, Jorgensen N, Ashburn P, Booker GR. J Appl Phys 1987;61:225.
[15] Liou BW, Lee CL, Lei TF, Wu YH. Jpn J Appl Phys Part 1 1997;36:3389.
[16] Chu TL, Chu SS, Vanderleen GA, Lin CJ, Boyd JR. Solid-State Electron 1978;21:781.